END
DATE
FILMED

6—80

DTIC

LEVEL

Office of Naval Research

Contract NC0014-77-C-0417

Task No. NR053-645

Technical Report No. 7

Molecular Dynamics of Mixed-Metal Clusters. ^{13}C and ^{1}H NMR

Studies of $H_2FeRu_3(CO)_{13}$, $H_2FeRu_2Os(CO)_{13}$, and $H_2FeRuOs_2(CO)_{13}$

by

Wayne L. Gladfelter and Gregory L. Geoffroy*

Prepared for Publication

in

Inorganic Chemistry

Department of Chemistry
The Pennsylvania State University
University Park, Pennsylvania 16802

April 25, 1980

80   5   6   001

REPORT DOCUMENTATION PAGE		READ INSTRUCTIONS BEFORE COMPLETING FORM
1. REPORT NUMBER Technical Report No. 7	2. GOVT ACCESSION NO. AD-A084356	3. RECIPIENT'S CATALOG NUMBER
4. TITLE (and Subtitle) Molecular Dynamics of Mixed-Metal Clusters. (^{13}C and ^{1}H NMR Studies of $H_2FeRu_3(CO)_{13}$, $H_2FeRu_2Os(CO)_{13}$, and $H_2FeRuOs_2(CO)_{13}$.		5. TYPE OF REPORT & PERIOD COVERED Interim Technical Report
		6. PERFORMING ORG. REPORT NUMBER N00014-77-C-0417
7. AUTHOR(s) Wayne L. Gladfelter and Gregory L. Geoffroy		8. CONTRACT OR GRANT NUMBER(s) N00014-77-C-0417
9. PERFORMING ORGANIZATION NAME AND ADDRESS Department of Chemistry The Pennsylvania State University University Park, PA 16802		10. PROGRAM ELEMENT, PROJECT, TASK AREA & WORK UNIT NUMBERS NR053-645
11. CONTROLLING OFFICE NAME AND ADDRESS		12. REPORT DATE 25 Apr 80
		13. NUMBER OF PAGES 35
14. MONITORING AGENCY NAME & ADDRESS(if different from Controlling Office)		15. SECURITY CLASS. (of this report) Unclassified
		15a. DECLASSIFICATION/DOWNGRADING SCHEDULE

16. DISTRIBUTION STATEMENT (of this Report)

Distribution unlimited; approved for public release

17. DISTRIBUTION STATEMENT (of the abstract entered in Block 20, if different from Report)

TR-7

18. SUPPLEMENTARY NOTES

Accepted for publication in Inorganic Chemistry

19. KEY WORDS (Continue on reverse side if necessary and identify by block number)

^{1}H NMR	$H_2FeRu_3(CO)_{13}$	$H_2FeRuOs_2(CO)_{13}$
^{13}C NMR	$H_2FeRu_2Os(CO)_{13}$	Fluxional

20. ABSTRACT (Continue on reverse side if necessary and identify by block number)

Variable temperature ^{1}H and ^{13}C NMR spectra of $H_2FeRu_3(CO)_{13}$, $H_2FeRu_2Os(CO)_{13}$, and $H_2FeRuOs_2(CO)_{13}$ have been measured and interpreted in view of three distinct fluxional processes. In the lowest temperature

DD FORM 1473 EDITION OF 1 NOV 65 IS OBSOLETE
1 JAN 73
S/N 0102-LF-014-6601

process the bridging and terminal carbonyls bound to Fe undergo localized exchange. The second process involves migration of the carbonyls around the face of the tetrahedral cluster that contains the bridging carbonyls. The highest temperature process involves a subtle reorganization of the metal framework. This latter process accounts for interconversion of the two enantiomers of the C_1 isomer of $H_2FeRu_2Os(CO)_{13}$ and $H_2FeRuOs_2(CO)_{13}$ and allows for the $C_s \rightleftarrows C_1$ isomerization. Lineshape analysis of the ^1H NMR spectra and comparison of the ^{13}C NMR spectra show that the activation barriers for each process increases as the Os content of the cluster increases.

Introduction

Metal clusters have been shown to undergo a wide variety of fluxional processes in which carbonyls, hydrides, and even the metals themselves undergo rearrangement.[1] Mixed-metal clusters are ideally suited for studies of the fluxional processes of clusters because of the low symmetry which is inherent within their metal framework. In such clusters, the majority of ligands are in chemically non-equivalent positions and are thus distinguishable by NMR spectroscopy.[2] Furthermore, a homologous series of mixed-metal clusters allows one to study the effects of metal substitution on the fluxional processes and their activation parameters.

In a preliminary communication we reported the results of a ^{13}C NMR study of $H_2FeRu_3(CO)_{13}$ and $H_2FeRuOs_2(CO)_{13}$ in which three distinct fluxional processes were observed, with the highest activation process involving a subtle rearrangement of the metal framework of each cluster.[3] The full details of the ^{1}H NMR spectra of these two clusters are described herein along with the ^{1}H and ^{13}C NMR spectra of $H_2FeRu_2Os(CO)_{13}$. This last cluster completes the series and allows an assessment of the effect of progressive substitution of Os for Ru within the series.

Experimental

$H_2FeRu_3(CO)_{13}$, $H_2FeRu_2Os(CO)_{13}$, and $H_2FeRuOs_2(CO)_{13}$ were prepared by published procedures.[4] Enrichment of each of these compounds was accomplished by stirring hexane solutions of each under an atmosphere of 90% enriched ^{13}CO (Stohler Isotope Co.). Exact enrichment conditions varied: 70% enrichment of $H_2FeRu_3(CO)_{13}$ after stirring at 45-50°C for 140 h; 60% enrichment of $H_2FeRu_2Os(CO)_{13}$ after stirring at 25°C for 380 h; 40% enrichment of $H_2FeRuOs_2(CO)_{13}$ after stirring at 25°C for 181 h. The approximate percent enrichment was determined by mass spectrometry.
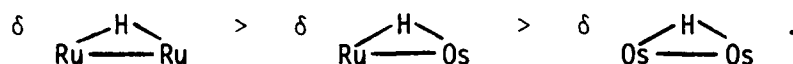
NMR spectra were recorded using 10 mm NMR tubes containing ∼3 mL of sample solution. Each tube was thoroughly degassed using freeze-pump-thaw techniques and then sealed under vacuum. Samples used for the ^{13}C NMR studies contained [$Cr(acac)_3$] (0.05 M) as a shiftless relaxation agent. The lock substance in each case was deuterated solvent. Spectra were recorded on a JEOL PS-100 FT NMR spectrometer equipped with a Nicolet 1080 computer for analysis. Heteronuclear decoupling was accomplished using a broad band noise decoupler. All reported ^1H and ^{13}C chemical shifts are relative to TMS. Line shape analyses were conducted on the Pennsylvania State University's IBM 370 computer utilizing the program DNMR3.[5] Infrared spectra were recorded on a Perkin Elmer 580 grating infrared spectrophotometer, and variable temperature IR spectra were recorded using an infrared cell manufactured by Harrick Scientific Corporation.

Results

The trimetallic clusters $H_2FeRu_2Os(CO)_{13}$ and $H_2FeRuOs_2(CO)_{13}$ each exists in the two isomeric forms shown in Figure 1. These will hereafter be denoted by their C_1 and C_s symmetry labels. The isomers of each cluster have not been separated, and indeed the ^{1}H NMR spectra discussed below show that the isomers readily interconvert at laboratory temperatures. Analysis of the bridging carbonyl region of the IR spectrum of each of the trimetallic clusters shows that at 25°C in hexane solution, the C_1 isomer of $H_2FeRu_2Os(CO)_{13}$ is in greater abundance than the C_s isomer whereas for $H_2FeRuOs_2(CO)_{13}$ the isomers are of about equal concentration.[4,6] Infrared spectroscopy also shows that the $C_s \rightleftarrows C_1$ equilibrium of $H_2FeRuOs_2(CO)_{13}$ shifts to the left upon cooling. We would ideally like to compare the values obtained at different temperatures for the equilibrium concentrations of the two isomers using IR and ^{1}H NMR spectroscopy. However, the resolution of the IR spectra and the necessity of using different solvents for the two studies[7] coupled with the likely solvent dependence of the $C_s \rightleftarrows C_1$ equilibrium has prevented us from obtaining meaningful results.

^{1}H NMR Spectra. The variable temperature ^{1}H NMR spectra of $H_2FeRu_2Os(CO)_{13}$ and $H_2FeRuOs_2(CO)_{13}$ are shown in Figures 2 and 3. In the low temperature limiting spectrum each cluster shows a singlet and a pair of doublets. The singlet is attributed to the two equivalent hydrogens of the C_s isomer while the pair of doublets are assigned to the two nonequivalent hydrogens of the C_1 isomer. Pertinent ^{1}H NMR spectral parameters for the limiting spectra are given in Table I. The average magnitude of the chemical shift (negative) for the $H_2FeRu_3(CO)_{13}$, $H_2FeRu_2Os(CO)_{13}$, and $H_2FeRuOs_2(CO)_{13}$ series increases as the Os content of the cluster increases, and for each

of the C_1 isomers we attribute the upfield doublet to the hydride which bridges the M-M bond with the greatest Os content. Indeed, the data given in Table I are fully consistent with the chemical shift ordering:

$$\delta \quad \underset{Ru\!-\!\!-\!\!-\!Ru}{\overset{\diagup H \diagdown}{}} \quad > \quad \delta \quad \underset{Ru\!-\!\!-\!\!-\!Os}{\overset{\diagup H \diagdown}{}} \quad > \quad \delta \quad \underset{Os\!-\!\!-\!\!-\!Os}{\overset{\diagup H \diagdown}{}} \quad .$$
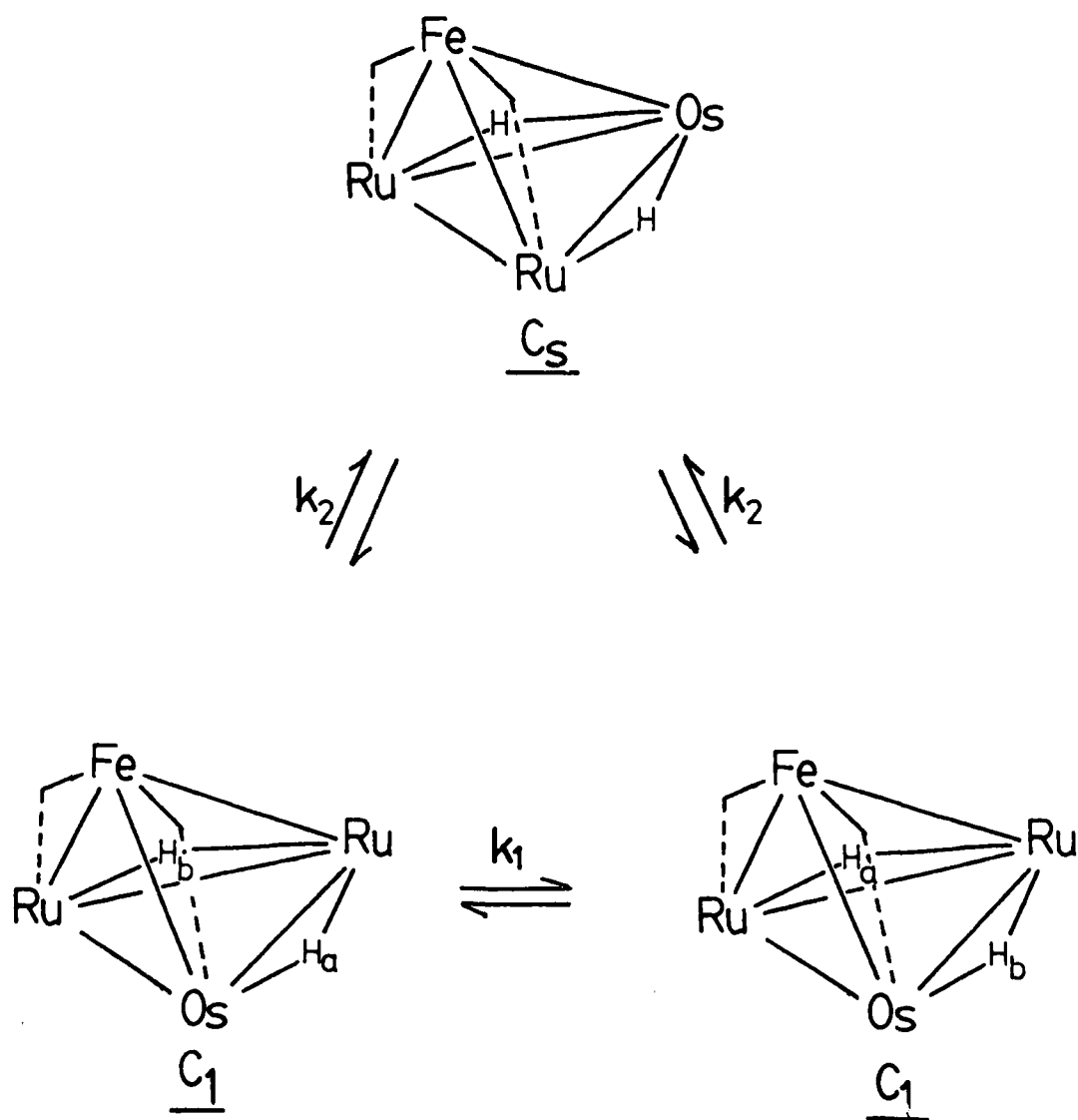
As the temperature is raised, the resonances in the spectra of each cluster broaden as the hydrogens begin to exchange positions, coalesce, and finally sharpen to a singlet at the high-temperature limit, Figures 2 and 3. The variable temperature spectra were computer-simulated using the model shown in Scheme 1 for $H_2FeRu_2Os(CO)_{13}$.

(Scheme 1 here)

It was necessary to include both processes shown in Scheme 1 which involve isomerization (k_2) and exchange of the two hydrogens of the C_1 isomer (k_1). Computer simulation using a single rate parameter (k), which might represent either of the processes shown in Scheme 1 or a constant ratio of the two processes, did not give a satisfactory fit to the experimental spectra. The kinetic parameters which were derived from the lineshape analyses are given in Table I, and a comparison of the calculated and experimental spectra of $H_2FeRuOs_2(CO)_{13}$ is shown in Figure 3. For both $H_2FeRu_2Os(CO)_{13}$ and $H_2FeRuOs_2(CO)_{13}$, the ^{1}H NMR spectra indicate that the isomerization process occurs with a lower activation energy than does hydrogen exchange localized on the C_1 isomer.

Scheme 1

The lineshape analysis requires a knowledge of the relative concentrations of the C_1 and C_s isomers at each temperature. These values were obtained by integration of spectra measured at temperatures below exchange followed by extrapolation to higher temperatures. The $C_s \rightleftarrows C_1$ equilibrium was observed to shift to the left upon cooling each cluster, in complete accord with the IR results mentioned above, and the ΔH and ΔS values obtained from measurement of the equilibrium constants at various temperatures are included in Table I.

Solubility problems prevented measurement of the spectra of H_2FeRu_2-$Os(CO)_{13}$ in the same solvent over the entire temperature range; $CDCl_3$ was employed above -8°C whereas an acetone-d_6/$CHCl_2F$ mixture was used at lower temperatures. Slight differences in the chemical shifts were noted in the two different solvents, and we were thus unable to model the exchange processes of this cluster over the entire temperature range. The $\Delta G^{\ddagger}$ values listed in Table I were obtained by simulating only the three lowest-temperature spectra and the rate constants obtained at -15°C were used for the $\Delta G^{\ddagger}$ calculation.

Low-Temperature Limiting ^{13}C NMR Spectra. The low-temperature limiting ^{13}C NMR spectra for $H_2FeRu_3(CO)_{13}$, $H_2FeRu_2Os(CO)_{13}$, and $H_2FeRuOs_2(CO)_{13}$ are shown in Figure 4. Figure 1 gives the labeling schemes used for assigning the observed resonances to specific carbonyls.

$H_2FeRu_3(CO)_{13}$ and $H_2FeRuOs_2(CO)_{13}$. The resonances in the low-temperature limiting spectra of $H_2FeRu_3(CO)_{13}$ and $H_2FeRuOs_2(CO)_{13}$ were assigned earlier in ref. 3 and the detailed rationale need not be repeated here. The specific assignments are summarized in Table II. Basically, three important factors were considered in developing these assignments. First, carbonyl ligands which are located trans to the hydride ligands show stronger [13]C-^{1}H coupling

than do carbonyls cis to the hydrides. Comparison of the ^{13}C and $^{13}C\{^1H\}$ spectra thus allows a determination of which resonances are due to CO's trans to the hydrides and which are not. Second, it was found that the terminal carbonyls bound to different metals group together in characteristic chemical shift regions. The chemical shift decreases relative to TMS upon descending the triad: Fe (204-211 ppm) > Ru (184-189 ppm) > Os (168-177 ppm). Third, for $H_2FeRuOs_2(CO)_{13}$ it was necessary to rely on information gained from its ^1H NMR spectrum which showed the C_s isomer to be more abundant than the C_1 isomer; thus the more intense resonances in the ^{13}C NMR spectra are assigned to the carbonyls on the C_s isomer.

$\underline{H_2FeRu_2Os(CO)_{13}}$. The assignment of the resonances in the ^{13}C NMR spectrum of $H_2FeRu_2Os(CO)_{13}$ is not as unambiguous as that for $H_2FeRuOs_2(CO)_{13}$, primarily because neither the C_s nor the C_1 isomer is dominant at low temperature and we cannot argue on the basis of relative intensity. Furthermore, the peak widths are broader in the $^{13}C\{^1H\}$ spectra of H_2FeRu_2-$Os(CO)_{13}$, Figure 5, making the comparison of the ^{13}C and $^{13}C\{^1H\}$ spectra difficult. The increased broadening is likely due to increased ^{13}C-^{13}C coupling since the $H_2FeRu_2Os(CO)_{13}$ cluster was enriched to 60% ^{13}CO compared to 40% enrichment for $H_2FeRuOs_2(CO)_{13}$.

As with $H_2FeRu_3(CO)_{13}$ and $H_2FeRuOs_2(CO)_{13}$, the carbonyl resonances in $H_2FeRu_2Os(CO)_{13}$ are grouped by metal, with the Os carbonyls in the 170-177 ppm range, the Ru carbonyls in the 185-193 ppm range, and the Fe carbonyls above 204 ppm. The resonances at 227, 232, and 213 ppm are respectively assigned to the bridging carbonyls $\underline{a}$, $\underline{i}$, and $\underline{j}$. These assignments are made primarily by a comparison to the spectra of $H_2FeRu_3(CO)_{13}$ and $H_2FeRuOs_2(CO)_{13}$: carbonyls $\underline{a}$ (227 ppm) of the C_s isomer of $H_2FeRu_2Os(CO)_{13}$ both bridge Fe-Ru bonds and hence are in similar chemical environments as $\underline{a}$

in $H_2FeRu_3(CO)_{13}$ (229 ppm); carbonyl $\underline{i}$ of $H_2FeRu_2Os(CO)_{13}$ (232 ppm) and $\underline{i}$ of $H_2FeRuOs_2(CO)_{13}$ (229 ppm) also both bridge Fe-Ru bonds and hence have similar chemical shifts; carbonyl $\underline{j}$ of $H_2FeRu_2Os(CO)_{13}$ (213 ppm) and $\underline{j}$ of $H_2FeRuOs_2(CO)_{13}$ (211 ppm) both bridge Fe-Os bonds. As with the terminal carbonyls, the bridging carbonyls that are associated with Os occur upfield of those associated with only Fe or Ru.
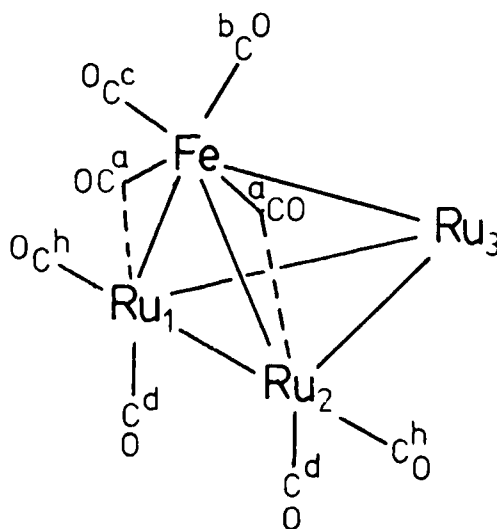
Resonances attributed to the terminal Fe carbonyls of $H_2FeRu_2Os(CO)_{13}$ ($\underline{b}$, $\underline{c}$, $\underline{k}$, $\underline{l}$) are at 211 and 204 ppm. These resonances cannot be specifically assigned but each is apparently the sum of two accidentally equivalent resonances, one from each isomer. Their chemical shifts compare well to those of $H_2FeRu_3(CO)_{13}$ (211 and 203 ppm) and $H_2FeRuOs_2(CO)_{13}$ (C_s, 211 and 204 ppm; C_1, 210 and 201 ppm).

Five non-equivalent carbonyls are bound to Os in the two isomers (C_s, $\underline{d}$ and $\underline{e}$; C_1, $\underline{p}$, $\underline{q}$, and $\underline{t}$) and four resonances are clearly observed in the 170-177 ppm range. The large resonance at 173 ppm apparently arises from two signals. The peak at 174 ppm is the only one obviously affected by ^1H coupling, indicating it is either $\underline{e}$ on the C_s isomer or $\underline{t}$, on the C_1 isomer. At -20°C, before the onset of isomerization, this is one of the three remaining Os carbonyl resonances, Figure 5. On the basis of the exchange processes that occur in $H_2FeRu_3(CO)_{13}$ and $H_2FeRuOs_2(CO)_{13}$ (<u>vide infra</u>) these three carbonyls would be $\underline{d}$ and $\underline{e}$ on the C_s isomer and $\underline{t}$ on the C_1 isomer. It is also apparent that at this temperature the 174 ppm resonance has increased in intensity relative to the other Os carbonyls. Recalling that the $C_s \rightleftarrows C_1$ equilibrium shifts to the right with increasing temperature, this carbonyl must be bound to the C_1 isomer and is therefore attributed to carbonyl $\underline{t}$. At this temperature, the 170 and 173 ppm resonances show a 1:2 intensity ratio and are assigned to carbonyls $\underline{d}$ and $\underline{e}$, respectively.
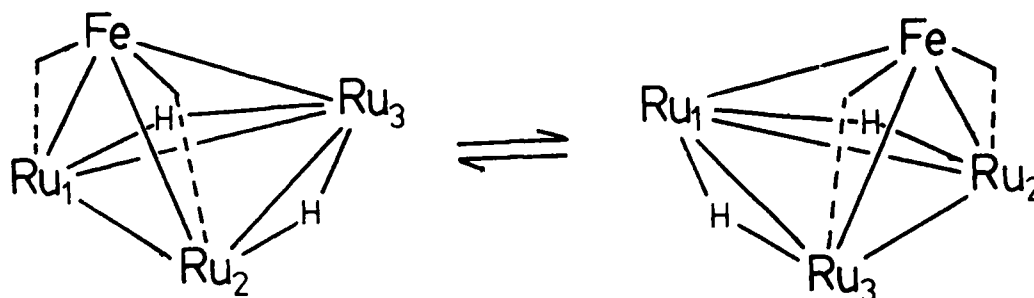
The second peak at 173 ppm and the peak at 177 ppm must be assigned to carbonyls p̲ and q̲.

We are unable to definitively assign the resonances due the Ru bound carbonyls. However, five resonances remain in the Ru carbonyl region in the -20°C spectrum, Figure 5, and based on the fluxional processes discussed below, these should correspond to carbonyls h̲ on the C_s isomer and o̲, r̲, s̲, and u̲, on the C_1 isomer. Of these five resonances, the peak at 188 ppm decreases in intensity relative to the others as the temperature is raised, indicating that it is due to carbonyl h̲ on the C_s isomer.

Carbonyl Exchange Processes. $H_2FeRu_3(CO)_{13}$. The variable temperature ^{13}C NMR spectra of $H_2FeRu_3(CO)_{13}$ were shown in Figure 1 of ref. 3 and the corresponding spectral changes were discussed therein. Here we simply summarize the main features of those results. As the temperature is raised from the low-temperature limiting spectrum at -95°C, resonances due to carbonyls a̲, b̲, and c̲ collapse, indicating the occurrence of bridge-terminal interchange localized on Fe as the first process. Before these peaks disappear completely, a second fluxional process begins at -65°C and averages resonances due to carbonyls a̲, b̲, c̲, d̲, and h̲. The most reasonable mechanism that would average these carbonyls involves their movement in a cyclic process about the $Fe-Ru_1-Ru_2$ plane.

The final fluxional process begins at -45°C and simultaneously averages the three remaining carbonyls $\underline{e}$, $\underline{f}$, and $\underline{g}$ with $\underline{a}$, $\underline{b}$, $\underline{c}$, $\underline{d}$, and $\underline{h}$. We have proposed[3] that this final exchange process occurs by a shift in the metal framework in which the Fe atom moves closer to Ru_3 and away from Ru_1 with a concomitant shift of the bridging carbonyls and one bridging hydrogen. This generates a structure completely identical with the initial structure but in which the $Fe-Ru_2-Ru_3$ triangle now possesses the bridging carbonyls.

A cyclic process, identical with that described above, can now occur around the $Fe-Ru_2-Ru_3$ plane. A third equivalent shift would allow a cyclic process around the $Fe-Ru_1-Ru_2$ plane. These equivalent shifts and the resultant cyclic movements will have the effect of averaging all the carbonyls in the molecule. An alternate final exchange process, consistent with the observed NMR changes, would involve localized scrambling on Ru_3 coupled with a cyclic process around the $Ru_1-Ru_2-Ru_3$ triangle. Although these two possible mechanisms cannot be distinguished for $H_2FeRu_3(CO)_{13}$, the NMR data discussed below for $H_2FeRuOs_2(CO)_{13}$ unambiguously show that the exchange in the latter cluster occurs by the intrametallic rearrangement process.[3]

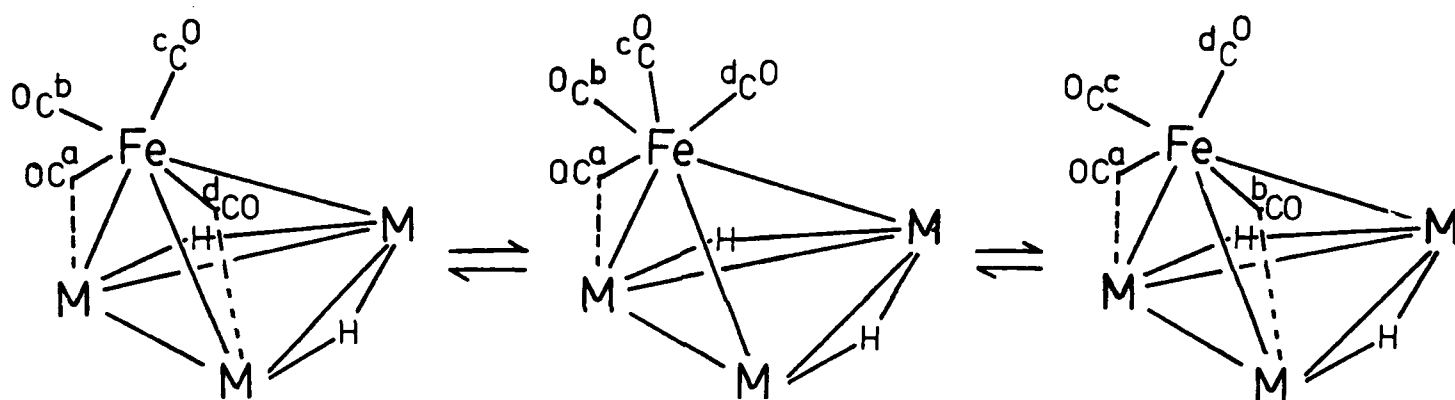$\underline{H_2FeRuOs_2(CO)_{13}}$. The variable temperature ^{13}C NMR spectra of $H_2FeRuOs_2(CO)_{13}$ are shown in Figure 6. As the temperature is raised, three

basic carbonyl exchange processes appear. As for $H_2FeRu_3(CO)_{13}$, the bridging and terminal Fe carbonyls exchange in the lowest temperature process. These Fe carbonyl resonances are fully broadened by -40°C in the C_1 isomer, while those in C_s are not broadened until -20°C. The second process, exactly analogous to that in $H_2FeRu_3(CO)_{13}$, averages carbonyls $\underline{i}$-$\underline{m}$, $\underline{p}$, $\underline{q}$, and presumably $\underline{n}$ of C_1 and carbonyls $\underline{a}$-$\underline{c}$, $\underline{f}$, and $\underline{g}$ of C_s through a cyclic movement of the carbonyls around the plane that originally contained the bridging carbonyls. Again, C_1 begins this process about 40° before C_s.

The third fluxional process can be rationalized as a shift in the metal framework similar to that discussed above for $H_2FeRu_3(CO)_{13}$. In the C_1 isomer this process begins at 10°C at which point the resonances due to carbonyls $\underline{o}$, $\underline{s}$, and presumably $\underline{r}$ begin to average. The resonances of carbonyls $\underline{t}$ and $\underline{u}$ do not collapse, but importantly they do become equivalent. This is readily explained by a rearrangement of the metal framework and associated ligands in which the Fe atom moves closer to Os_2 and away from Os_1. This, in effect, generates the enantiomer of the first structure and represents a racemization process.

The Fe-Ru-Os_2 triangle now possesses the bridging carbonyls. A cyclic process around this triangle averages $\underline{o}$, $\underline{s}$, and $\underline{r}$ with $\underline{i}$, $\underline{j}$, $\underline{k}$, and $\underline{l}$. Coupling of the intrametallic rearrangement with the cyclic processes has the net effect of averaging carbonyls $\underline{i}$-$\underline{s}$. Carbonyls $\underline{t}$ and $\underline{u}$, however, do not

enter into this exchange. As illustrated in Scheme 2, this rearrangement

Scheme 2

has the effect of showing an average environment to $\underline{t}$ and $\underline{u}$, and the
observation that $\underline{t}$ and $\underline{u}$ become equivalent provides strong support for
this mechanism.

The second effect of the intrametallic rearrangement in C_1 occurs
when the Fe atom moves away from Ru and generates the $Fe-Os_1-Os_2$ triangle
with the bridging CO's. This movement results in isomerization to the C_s
isomer and is the final averaging process. It begins at 40°C and results
in the averaging of all carbonyls on both isomers. Importantly, these [13]C
NMR spectra clearly indicate that racemization occurs prior to isomerization
in the averaging of all carbonyls on both isomers.

$\underline{H_2FeRu_2Os(CO)_{13}}$. The variable temperature ^{13}C NMR spectra of
$H_2FeRu_2Os(CO)_{13}$ are shown in Figure 5. As in $H_2FeRuOs_2(CO)_{13}$, the two
isomeric forms act separately in each of the exchange processes. At -70°C,
the Fe carbonyls $\underline{a}$, $\underline{b}$, and $\underline{c}$ have coalesced on the C_s isomer. The analogous
process on the C_1 isomer occurs at -40°C. Since it was not possible to
definitively assign all the resonances in the low-temperature limiting
spectrum to specific carbonyls, it is difficult to unambiguously distinguish
the next processes to occur. However, the lack of changes in the Os-CO
region between -40°C and -70°C and the lack of appearance of an averaged

Fe-CO resonance are consistent with exchange of the carbonyls in a cyclic path around the Fe-Ru$_1$-Ru$_2$ face of the C$_s$ isomer. Above -40°C, peaks due to carbonyls $\underline{m}$, $\underline{n}$, and $\underline{p}$ coalesce with the Fe carbonyl resonances. This process must involve the movement of carbonyls around the Fe-Ru-Os face of the C$_1$ isomer. At 0°C, there begins a general decrease in intensity of all resonances to give coalescence and what appears to be a single resonance growing in at 193 ppm in the 70°C spectrum.

Discussion

CO Exchange Mechanisms. Three distinctly different CO exchange
processes are resolved for these mixed-metal clusters.   The
first process to occur at the lowest temperatures is exchange of the bridging
and terminal carbonyls bound to Fe. A reasonable mechanism for this
exchange is shown in Scheme 3 and involves opening of one of the carbonyl

Scheme 3

bridges, a subsequent trigonal twist of the resultant $Fe(CO)_3$ unit, and
finally reformation of the CO bridge. A consequence of this mechanism is that
the bridging CO's should decrease in intensity less rapidly than the
terminal CO's since the twist must occur twice in order for exchange of
both bridging CO's to occur. This suggestion is most strongly supported by
the $H_2FeRu_3(CO)_{13}$ spectra shown in Figure 1 of ref. 3. At -55°C the
bridging CO resonance is clearly visible while the terminal CO resonances
have collapsed into the baseline.

The next exchange process to occur at slightly higher temperatures
involves migration of the carbonyls around the Fe-M-M triangle which

possesses the bridging carbonyls. It seems reasonable to propose that the intermediates in this cyclic movement are the tautomers which have the semi-bridging carbonyls bound mainly to Ru or Os atoms instead of Fe as indicated in Scheme 4. During the occurence of this process, the hydrogens remain in their original positions. This is consistent with the observed ^{1}H NMR spectra of $H_2FeRu_2Os(CO)_{13}$ and $H_2FeRuOs_2(CO)_{13}$ since

Scheme 4

racemization, the net effect of hydrogen movement, does not occur in the temperature range in which the ^{13}C NMR spectra shows the cyclic fluxional processes.

A number of di- and polynuclear complexes have been shown to undergo similar cyclic exchange processes.[8-12] Cotton and coworkers[8,9] have suggested that coplanarity is not a mandatory requirement for the ligands that participate in such a process but only that the path be continuous and closed. This requirement is certainly fulfilled in these clusters and furthermore the crystal structure of $H_2FeRu_3(CO)_{13}$[13] does indicate that 7 of the 8 carbonyls involved are indeed virtually coplanar. The only exception is one of the terminal carbonyls attached to Fe, but by the time the cyclic process begins to occur, this carbonyl is rapidly exchanging with the bridging CO's.

The third and final process to occur is one which involves a shift in the metal framework and which accounts for racemization, isomerization and total exchange of all the carbonyl ligands. This process and its implications are best illustrated by consideration of the drawings in Scheme 5 which depict the metal framework of $H_2FeRuOs_2(CO)_{13}$, the two bridging CO's and the two bridging hydrides. The asymmetry of the cluster is grossly exaggerated for clarity. The process basically involves movement of the iron away from one metal and closer to another with a concomitant shift of the bridging carbonyls. It also involves a slight elongation or compression of all the M-M bonds, and it must be accompanied by a shift in position of one of the bridging hydrides.

Referring to Scheme 5 and starting with the C_{1_a} enantiomer, if the Fe moves away from Os_1 towards Os_2, it generates the C_{1_b} enantiomer. This process leads to racemization since H_B must also shift in the process. Movement of Fe away from Ru in either of the C_1 enantiomers and toward both Os atoms leads to the C_s isomer and accounts for the isomerization process. Each time the cluster rearranges, the carbonyls execute the cyclic process about a different Fe-M-M face and hence involve different carbonyl ligands in that process. The cyclic processes coupled with the framework rearrangement leads to total exchange of all the carbonyl ligands.

The ^{13}C and ^1H NMR spectra of $H_2FeRuOs_2(CO)_{13}$ indicate that two distinct hydrogen migration processes occur for the C_1 isomer. Only one of these involves actual exchange of the two hydrogens on the C_1 isomer, and, thus, is the only one detected in the ^1H NMR experiments.

SCHEME 5

The lower temperature, and hence lower activation energy, process is that specifically depicted in Scheme 5 which involves migration of only one hydrogen atom. The hydrogen which bridges the $Ru-Os_2$ bond (H_B) could simply move across the $Ru-Os_1-Os_2$ triangle to bridge the $Ru-Os_1$ bond. No exchange occurs with H_A which bridges the Os-Os bond and hence this movement would not be detected in the ^1H NMR spectrum. However, this process does necessitate a concerted shift in the metal framework and is thus detected by ^{13}C NMR, and it, of course, does lead to racemization, Scheme 2.

An estimate of $\Delta G^{\ddagger}$ for this process can be obtained by careful examination of the behavior of carbonyls $\underline{t}$ and $\underline{u}$ in the variable temperature NMR spectrum, Figure 6. As shown in Scheme 2, carbonyls $\underline{t}$ and $\underline{u}$ become equivalent during this exchange process, but they do not exchange with any of the other carbonyls. This system can thus be treated as an isolated two site exchange problem in which both sites are equally populated. A reasonable estimate of $\Delta G^{\ddagger}$, obtained simply from the chemical shift difference of carbonyls $\underline{t}$ and $\underline{u}$ (15 hz; 100 Mhz instrument) and their coalesence temperature (10°C), is 15 kcal/mole.

The second, higher-temperature, and hence higher-activation energy process that is detectable by ^1H NMR spectroscopy is that depicted in Scheme 6.

Scheme 6

$\underline{C}_{1a}$ $\underline{C}_{1b}$

In this process both hydrogens move through an intermediate in which they are each terminally bound to the two Os atoms. This intermediate could collapse as shown in Scheme 6 to give either C_{1a} or C_{1b}. Note that this process must also be accompanied by a concomitant shift in the metal framework. In this scheme, H_A and H_B exchange each time the framework shift occurs. For $H_2FeRuOs_2(CO)_{13}$, $\Delta G^{\ddagger}_{283} = 17.8$ kcal/mole for this process, compared to the $\Delta G^{\ddagger}_{283}$ value of 15 kcal/mole for the first process.

Effect of Variations in the Metal Framework. Although within the series $H_2FeRu_3(CO)_{13}$, $H_2FeRu_2Os(CO)_{13}$, and $H_2FeRuOs_2(CO)_{13}$ the exchange processes are identical, <u>the activation barrier for each process increases</u> <u>as the osmium content of the cluster increases</u>. We are not able to unambiguously rationalize this trend but a similar increase in activation energy in moving from Ru to Os has been noted for the series of monomeric $[M\{P(OR)_3\}_5]$ (M = Ru, Os) complexes studied by English and coworkers.[14] It is unlikely that the activation energy increase can be accounted for solely on the basis of a size increase in the metal involved in the fluxional process since Ru and Os probably have similar atomic radii in these clusters. In $Ru_3(CO)_{12}$ and $Os_3(CO)_{12}$, for example, the metal atomic radii are 1.43 Å and 1.44 Å, respectively.[15] On the other hand, Os certainly possesses a greater amount of electron density than does Ru and this could be the important factor in determining the activation energies.

An interesting comparison can be made to the homonuclear cluster $H_2Ru_4(CO)_{13}$, 4, which is isostructural with the mixed-metal clusters reported herein.[16] The exchange processes which this cluster undergoes have been found by Milone and coworkers[17] to be quite similar to those of the mixed-metal analogs. However, bridge-terminal interchange localized on Ru_1 is not the lowest temperature process in $H_2Ru_4(CO)_{13}$, but instead

4

the cyclic exchange of CO's around the Ru_1-Ru_2-Ru_3 face occurs rapidly

even at -72°C. It was proposed that the lower activation barrier observed

for $H_2Ru_4(CO)_{13}$ compared to $H_2FeRu_3(CO)_{13}$ results from the increased

stability of bridging carbonyls bound to first row metals.[17] This

proposal is further supported here. In Scheme 4 the intermediates 2 and 3

have one of the bridging carbonyls bridging either a Ru-Ru, Ru-Os, or

an Os-Os bond. The least favorable case would involve migration of the

CO's around the Fe-Os_1-Os_2 face of the C_s isomer of $H_2FeRuOs_2(CO)_{13}$.

Accordingly, we find this to have the highest activation barrier observed

for the cyclic process in any of the clusters. The energy difference between

the tautomers 1, 2, and 3 in Scheme 4 is least in the case where all the

metals are Ru and is greatest when one metal is Fe and the other two are Os.

Intrametallic Rearrangement. The last exchange process in $H_2FeRu_3(CO)_{13}$

and the last two processes in $H_2FeRuOs_2(CO)_{13}$ and $H_2FeRu_2Os(CO)_{13}$ involve

reorganization of the metal framework. The actual magnitude of the shifts

within the framework is relatively small, yet it still significantly

contributes to the final averaging process. The metal framework of $H_2FeRu_3(CO)_{13}$ is shown below with the average metal-metal bond distances derived from the reported crystal structure.[13] These values indicate that the greatest change that would occur in any one bond length during the rearrangement is 0.11 Å. We tend to view the reorganization process as more of a breathing motion of the metal framework, but one which has coupled to it motions of the carbonyl and hydride ligands.

It appears that intrametallic rearrangement processes are not at all uncommon, as noted by Band and Muetterties[1] in a recent review, but they are still poorly understood. In our case we would particularly like to understand how the various motions contribute to the overall rearrangement process; for example, what percentage of the 15.6 kcal/mole activation barrier for isomerization of $H_2FeRuOs_2(CO)_{13}$ is due to reorganization of the metal framework and what percentage is due to hydrogen migration? We expect that such matters will be the subject of future publications from this and other research groups.

References and Notes

1. Band, E.; Muetterties, E. L. Chem. Rev., 1978, 78, 639.

2. Gladfelter, W. L.; Geoffroy, G. L. Adv. Organomet. Chem., 1980, 18, in press.

3. Geoffroy, G. L.; Gladfelter, W. L. J. Am. Chem. Soc., 1977, 99, 6775.

4. Geoffroy, G. L.; Gladfelter, W. L. J. Am. Chem. Soc., 1977, 99, 7565.

5. Kleier, D. A.; Binsch, G. "DNMR3: A Computer Program for the Calculation of Complex Exchange-Broadened NMR Spectra. Modified Version for Spin Systems Exhibiting Magnetic Equivalence or Symmetry," Program 1065, Quantum Chemistry Program Exchange, Indiana University, Bloomington, Indiana.

6. The bridging ν_{CO} region of the spectra of $H_2FeRu_2Os(CO)_{13}$ and $H_2FeRuOs_2(CO)_{13}$ are shown in Figure 4 of ref. 4. For $H_2FeRu_2Os(CO)_{13}$ the bands at 1887 and 1861 cm^{-1} are attributed to the C_s isomer while the 1877 and 1849 cm^{-1} bands are those of the C_1 isomer. For $H_2FeRuOs_2(CO)_{13}$, the C_1 bands are 1882 and 1855 cm^{-1} and the C_s bands are 1870 and 1842 cm^{-1}. The rationale for these assignments are given in the text of ref. 4.

7. Saturated hydrocarbon solvents are required to obtain high resolution IR spectra; the clusters are not sufficiently soluble in hydrocarbons for high-quality NMR spectra.

8. Cotton, F. A.; Hanson, B. E.; Jamerson, J. D.; Stultz, B. R. J. Am. Chem. Soc., 1977, 99, 3293.

9. Cotton, F. A.; Haines, R. J.; Hanson, B. E.; Sekutowski, J. C. Inorg. Chem., 1978, 17, 2010.

10. Johnson, B. F. G.; Lewis, J.; Reichert, B. E.; Schorpp, K. T. J. Chem. Soc. Dalton Trans., 1976, 1403.

11. Tachikawa, M.; Richter, S. I.; Shapley, J. R. J. Organomet. Chem., 1977, 128, C9.

12. Martinengo, S.; Heaton, B. T.; Goodfellow, R. J.; Chini, P. J. Chem. Soc., Chem. Commun., 1977, 39.

13. Gilmore, C. J.; Woodward, P. J. Chem. Soc., A, 1971, 3453.

14. English, A. D.; Ittel, S. D.; Tolman, C. A.; Meakin, P., Jesson, J. P. J. Am. Chem. Soc., 1977, 99, 117.

15. Churchill, M. R.; Hollander, F. J.; Hutchinson, J. P. Inorg. Chem., 1977, 16, 2655.

16. Yawney, D. B. W.; Doedens, R. J. Inorg. Chem., 1972, 11, 838.

17. Aime, S.; Milone, L.; Osella, D.; Sappa, E. Inorg. Chim. Acta, 1978, 29, L211.

Table I. ^{1}H NMR Spectral Data, Activation, and Thermodynamic Parameters

Cluster	δ ppm	Activation Parameters		Thermodynamic Parameters
		Isomerization	$C_1 : H_A-H_B$ Exchange	$C_s \rightleftarrows C_1$
$H_2FeRu_3(CO)_{13}$ ^{a}	-18.4 s	---	---	---
$H_2FeRu_2Os(CO)_{13}$ ^{b}	-18.56 d (J_{H-H} = 1.65 hz)	$\Delta G^{\ddagger}_{258}$ = 14.2 kcal/mole	$\Delta G^{\ddagger}_{258}$ = 15.4 kcal/mole	ΔH = 0.4 kcal/mole
	-18.75 s			ΔS = 3.3 cal/mole-K
	-18.83 d (J_{H-H} = 1.65 hz)			
$H_2FeRuOs_2(CO)_{13}$ ^{a}	-19.55 s	$\Delta H^{\ddagger}$ = 15.6 $\pm$ 0.4 kcal/mole	$\Delta H^{\ddagger}$ = 15.0 $\pm$ 0.9 kcal/mole	ΔH = 0.9 kcal/mole
	-19.65 d (J_{H-H} = 1.27 hz)	$\Delta S^{\ddagger}$ = -6.1 $\pm$ 1.2 cal/mole-K	$\Delta S^{\ddagger}$ = -9.8 $\pm$ 2.8 cal/mole-K	ΔS = 3.0 cal/mole-K
	-19.82 d (J_{H-H} = 1.27 hz)	$\Delta G^{\ddagger}_{258}$ = 17.1 $\pm$ 0.7 kcal/mole	$\Delta G^{\ddagger}_{258}$ = 17.5 $\pm$ 1.2 kcal/mole	

^{a}CDCl$_3$ solution.

^{b}Acetone-d$_6$/CHCl$_2$F solution.

Table II. Assignment of the Low-Temperature Limiting ^{13}C NMR Spectra of $H_2FeRu_3(CO)_{13}$, $H_2FeRu_2Os(CO)_{13}$, and $H_2FeRuOs_2(CO)_{13}$ [a]

Cluster	Carbonyl (δ (ppm))
$H_2FeRu_3(CO)_{13}$ [b]	a (229); b,c (203, 211); d,h (193, 186.7); e,f (190.2, 189.9); g (187)
$H_2FeRu_2Os(CO)_{13}$	**C_s isomer** a (227); b,c (211, 204); d (170); e (173); f,g (188[c], 188[c]); h (188[c]) **C_1 isomer** i (232); j (213); k,l (211, 204); m,n (193, 188[c]); p,q (173, 177); o,r,s,u (189.5, 188.9, 187, 186); t (174)
$H_2FeRuOs_2(CO)_{13}$ [b]	**C_s isomer** a (217); b,c (204, 211); d (188); e (185); f,g (174.5, 174.9); h (172) **C_1 isomer** i (229); j (211); k,l (201, 210); m,n (188, 189); o (184); p (177); q (174); r (172); s (170); t,u (168, 169)

[a] See Figure 1 for labeling schemes. Resonances grouped together cannot be individually assigned to the indicated carbonyls.

[b] Ref. 3.

[c] This value is approximate due to overlap of several resonances in this region.

Figure Captions

Figure 1.   Carbonyl labeling schemes for $H_2FeRu_3(CO)_{13}$ and the C_s and C_1 isomers of $H_2FeRu_2Os(CO)_{13}$ and $H_2FeRuOs_2(CO)_{13}$.

Figure 2. ^1H NMR spectra of $H_2FeRu_2Os(CO)_{13}$. Spectra at $-41°C$, $-35°C$, and $-15°C$ were recorded in an acetone-d_6/$CHCl_2F$ solvent mixture while those above $-15°$ were obtained in $CDCl_3$.

Figure 3. ^1H NMR spectra of $H_2FeRuOs_2(CO)_{13}$ recorded in $CDCl_3$ solution.

Figure 4.   Low-temperature limiting ^{13}C NMR spectra of a) $H_2FeRu_3(CO)_{13}$ ($-95°C$), b) $H_2FeRu_2Os(CO)_{13}$ ($-90°C$), and c) $H_2FeRuOs_2(CO)_{13}$ ($-60°C$).

Figure 5. ^{13}C NMR spectra of $H_2FeRu_2Os(CO)_{13}$. The resonances at 201.1 and 200.6 ppm which average to the 192.2 ppm resonance and which are marked with an asterisk are due to $Ru_2Os(CO)_{12}$ impurity which arises from decomposition of $H_2FeRu_2Os(CO)_{12}$ during the enrichment process. This was confirmed by isolating $Ru_2Os(CO)_{12}$ and determining its spectrum. The numbered resonances in the $-90°C$ spectrum are attributed to carbonyls which cannot be distinguished: (1) b, c, k, l; (2) see text; (3) e, p, q.

Figure 6. ^{13}C NMR spectra of $H_2FeRuOs_2(CO)_{13}$.

$H_2FeRu_3(CO)_{13}$

$H_2FeRu_2Os(CO)_{13}$

$\underline{C_S}$

$\underline{C_I}$

$H_2FeRuOs_2(CO)_{13}$
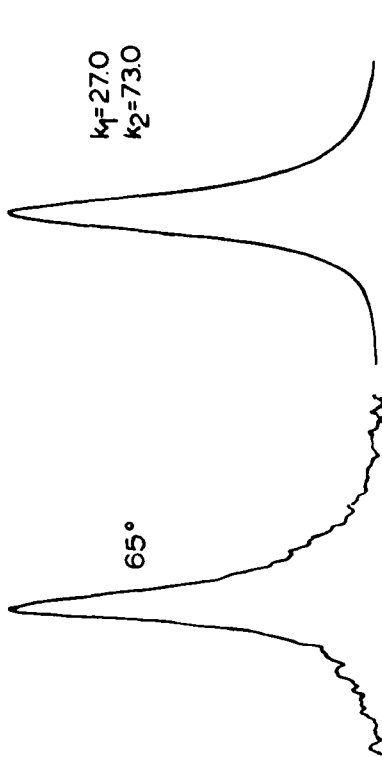
$\underline{C_S}$

$\underline{C_I}$

-8°

-15°

-35°

-41°

55°

39°

19°

10°

0°

28.9 ppm 29.2

28.9 ppm 29.2

$k_1 = 27.0$
$k_2 = 73.0$

$k_1 = 17.0$
$k_2 = 52.0$

$k_1 = 11.0$
$k_2 = 32.5$

$k_1 = 8.3$
$k_2 = 25.0$

$k_1 = 7.4$
$k_2 = 17.5$

65°

60°

55°

50°

45°

30.0

29.5   ppm

$k_1 = 5.1$
$k_2 = 12.4$

$k_1 = 4.0$
$k_2 = 8.5$

$k_1 = 2.2$
$k_2 = 6.1$

$k_1 = 1.8$
$k_2 = 3.5$

$k_1 = k_2 = 0$

40°

35°

31°

27°

10°C

C_1

C_S

30.0

29.5   ppm

(a)

a   b   c   d e,f g,h

(b)

i   a   j   l   l   2   3 3   t   e   d
                               f h

(c)

a   b   c   d   e   g   f h

i   j,k   ℓ   m,n o   p,q r s f,u

240   205   170

-50°

-70°

-80°

-90°

-90°
¹H-coupled

70°

30°

20°

0°

-20°

-30°

-40°

| 240 | 205 | 170 |
ppm

| 240 | 205 | 170 |
ppm

-20°C

-30°C

-40°C

-60°C

-60°C
¹H-coupled

240   200   160

108°C

80°C

60°C

30°C

20°C

10°C

0°C

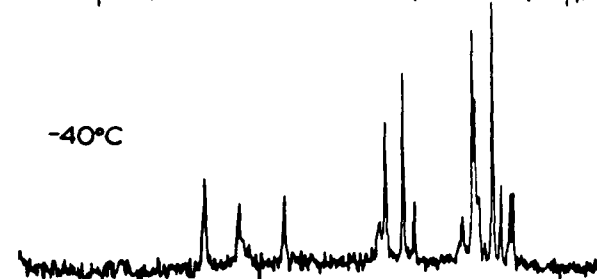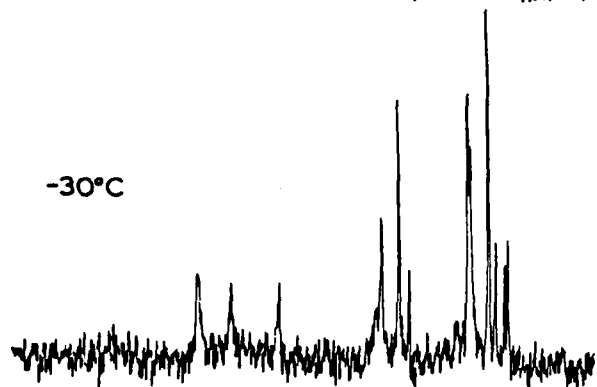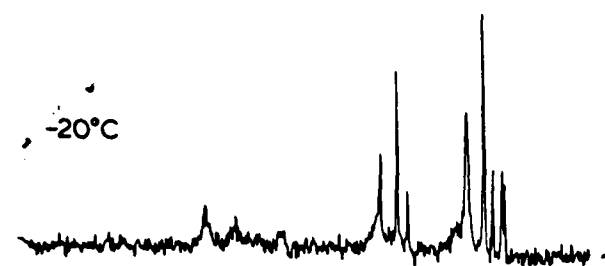240   200   160

TECHNICAL REPORT DISTRIBUTION LIST

No. Copies

No. Copies

Dr. R. M. Grimes
University of Virginia
Department of Chemistry
Charlottesville, Virginia 22901 1

Dr. M. Tsutsui
Texas A&M University
Department of Chemistry
College Station, Texas 77843   1

Dr. C. Quicksall
Georgetown University
Department of Chemistry
37th & O Streets
Washington, D.C. 20007   1

Dr. M. F. Hawthorne
University of California
Department of Chemistry
Los Angeles, California 90024 1

Dr. D. B. Brown
University of Vermont
Department of Chemistry
Arlington, Vermont 05401   1

Dr. W. B. Fox
Naval Research Laboratory
Chemistry Division
Code 6130
Washington, D.C. 20375   1

Dr. J. Adcock
University of Tennessee
Department of Chemistry
Knoxville, Tennessee 37916   1

Dr. A. Cowley
University of Texas
Department of Chemistry
Austin, Texas 78712   1

Dr. W. Hatfield
University of North Carolina
Department of Chemistry
Chapel Hill, North Carolina 27514   1

Dr. D. Seyferth
Massachusetts Institute of Technology
Department of Chemistry
Cambridge, Massachusetts 02139   1

Dr. M. H. Chisholm
Princeton University
Department of Chemistry
Princeton, New Jersey 08540   1

Dr. B. Foxman
Brandeis University
Department of Chemistry
Waltham, Massachusetts 02154   1

Dr. T. Marks
Northwestern University
Department of Chemistry
Evanston, Illinois 60201   1

Dr. G. Geoffrey
Pennsylvania State University
Department of Chemistry
University Park, Pennsylvania 16802 1

Dr. J. Zuckerman
University of Oklahoma
Department of Chemistry
Norman, Oklahoma 73019   1

TECHNICAL REPORT DISTRIBUTION LIST

No. Copies

Office of Naval Research
Arlington, Virginia 22217
Attn: Code 472   2

~~Office of Naval Research~~
~~Arlington, Virginia 22217~~
~~Attn: Code 102IP   1~~   ~~6~~

ONR Branch Office
536 S. Clark Street
Chicago, Illinois 60605
Attn: Dr. Jerry Smith   1

ONR Branch Office
715 Broadway
New York, New York 10003
Attn: Scientific Dept.   1

ONR Branch Office
1030 East Green Street
Pasadena, California 91106
Attn: Dr. R. J. Marcus   1

ONR Branch Office
760 Market Street, Rm. 447
San Francisco, California 94102
Attn: Dr. P. A. Miller   1

ONR Branch Office
666 Summer Street
Boston, Massachusetts 02210
Attn: Dr. L. H. Peebles   1

Director, Naval Research Laboratory
Washington, D.C. 20390
Attn: Code 6100   1

The Asst. Secretary of the Navy (R&D)
Department of the Navy
Room 4E736, Pentagon
Washington, D.C. 20350   1

Commander, Naval Air Systems Command
Department of the Navy
Washington, D.C. 20360
Attn: Code 310C (H. Rosenwasser) 1

No. Copies

Defense Documentation Center
Building 5, Cameron Station
Alexandria, Virginia 22314   12

U.S. Army Research Office
P.O. Box 12211
Research Triangle Park, N.C. 27709
Attn: CRD-AA-IP   1

Naval Ocean Systems Center
San Diego, California 92152
Attn: Mr. Joe McCartney   1

Naval Weapons Center
China Lake, California 93555
Attn: Head, Chemistry Division   1

Naval Civil Engineering Laboratory
Port Hueneme, California 93041
Attn: Mr. W. S. Haynes   1

Professor O. Heinz
Department of Physics & Chemistry
Naval Postgraduate School
Monterey, California 93940   1

Dr. A. L. Slafkosky
Scientific Advisor
Commandant of the Marine Corps (Code RD-1)
Washington, D.C. 20380   1

Office of Naval Research
Arlington, Virginia 22217
Attn: Dr. Richard S. Miller   1

ONR
Resident Representative
Room 407-MMCC
Carnegie-Mellon University
Pittsburgh, Pennsylvania   1